ground water

Biased Monitoring of Fresh Water–Salt Water Mixing Zone in Coastal Aquifers

by Eyal Shalev[1], Ariel Lazar[2,3], Stuart Wollman[2], Shushanna Kington[3], Yoseph Yechieli[2], and Haim Gvirtzman[3]

Abstract

In coastal aquifers, significant vertical hydraulic gradients are formed where fresh water and underlying salt water discharge together upward to the seafloor. Monitoring boreholes may act as "short circuits" along these vertical gradients, connecting between the higher and the lower hydraulic head zones. When a sea tide is introduced, the fluctuations of both the water table and the depth of the mixing zone are also biased due to this effect. This problem is intensified in places of long-screen monitoring boreholes, which are common in many places in the world. For example, all approximately 500 boreholes of the fresh water-salt water mixing zone in the coastal aquifer of Israel are installed with 10 to 50 m long screens. We present field measurements of these fluctuations, along with a three-dimensional numerical model. We find that the in-well fluctuation magnitude of the mixing zone is an order of magnitude larger than that in the porous media of the actual aquifer. The primary parameters that affect the magnitude of this bias are the anisotropy of the aquifer conductivity and the borehole hydraulic parameters. With no sea tide, borehole interference is higher for the anisotropic case because the vertical hydraulic gradients are high. When tides are introduced, the amplitude of the mixing zone fluctuation is higher for the isotropic case because the overall effective hydraulic conductivity is greater than the conductivity in the anisotropic case. In the aquifer, the fresh water-salt water mixing zone fluctuations are dampened, and tens of meters inland from the shoreline, the fluctuations are on the order of few centimeters.

Introduction

The interrelation between sea and coastal aquifers is of critical importance to the large human populations living in coastal areas. The interrelation involves the submarine ground water discharge (SGD) of relatively fresh water to the sea and the intrusion of sea water into the aquifer, which impairs the quality of ground water. This problem is important in Israel where the coastal aquifer is the country's third largest source of water. Because of the potentially irreversible damage of sea water intrusion, it is crucial that the mechanism governing the sea water intrusion process is better understood, such that policy makers can take the appropriate actions to protect this vital source of water. Therefore, accurate and reliable monitoring of sea water intrusion is critically important. All about 500 monitoring boreholes in the coastal aquifer of Israel are installed with 10- to 50-m-long screens. This study concentrates on biased monitoring of the fresh water-salt water mixing zone position in one of these boreholes.

Wellbore Flow in Long-Screen Borehole

Installation of monitoring boreholes may cause local vertical flow due to a natural vertical hydraulic gradient

[1]Corresponding author: Geological Survey of Israel, 30 Malkhe Israel, Jerusalem 95501, Israel; 972-2-5314-230; fax: 972-2-5380-688; eyal@gsi.gov.il

[2]Geological Survey of Israel, 30 Malkhe Israel, Jerusalem 95501, Israel.

[3]Institute of Earth Sciences, Hebrew University, Jerusalem 91904, Israel.

Received February 2008, accepted August 2008.

doi: 10.1111/j.1745-6584.2008.00502.x

at the well location (Church and Granato 1996). The borehole then acts as a "short circuit" along this gradient, connecting between the higher and lower hydraulic head zones (Elci et al. 2001). As a result, flow in the borehole (ambient flow) is often large enough to compromise the integrity of water samples and water table measurements. Until the 1980s, it was still argued that long-screen boreholes are more sensitive to the presence of different water bodies than short-screen wells because of better hydrologic connection with the aquifer and the ability to use discrete sampling based on electrical conductivity (EC) profiles (Giddings 1987). The presence of a well where in the transition zone between the water bodies was detected was used as a proof for the validity of the measurements (Giddings 1987). In addition, the high cost of more short-screen boreholes supports the argument of supporting long-screen boreholes.

Since the late 1980s, the use of long-screen boreholes for ground water sampling was countered in the literature by many studies, some of which are mentioned here. Shosky (1987) claimed that a long-screen borehole could penetrate different units with different permeabilities and thicknesses. If one of the units is contaminated, the contaminant will spread into the uncontaminated unit. Therefore, the use of borehole EC profiling to locate high-salinity zones is questionable. Robbins (1989) also showed with an analytical model that sampling from long-screen boreholes may underestimate the concentration of the contaminant because of dilution by flow from other units. Reilly et al. (1989) modeled numerically ambient flow in a long-screen borehole and concluded that, in some cases, long-screen wells are "almost useless" for measuring contaminants. They also pointed out that ambient flow may contaminate parts of the aquifer that would not otherwise become contaminated in the absence of long-screen boreholes. Konikow and Hornberger (2006) modeled preferential ground water flow through boreholes and showed that solute can be transported directly and quickly through long-screen boreholes. Lacombe et al. (1995) emphasized that abandoned and improperly sealed boreholes may act as conduits for contaminants. Church and Granato (1996) compared analyses of samples from short-screen and long-screen boreholes with borehole induction logs and concluded that samples from the long-screen boreholes are biased. Hutchins and Acree (2000) used an electromagnetic borehole flow meter and showed significant ambient flow. Elci et al. (2001) modeled the contamination caused by a long-screen borehole and showed that an artifact caused by ambient flow occurs even in homogeneous aquifers with small vertical hydraulic gradients. Elci et al. (2003) demonstrated that not only the salinity of the water in a borehole is diluted but also the hydraulic head measured in a long-screen borehole does not represent formation hydraulic head. However, Sukop (2000) claimed that data gathered from long-screened boreholes are not useless but are valuable for modeling flow and transport. He developed a relatively simple method to compute vertical distribution of solute concentration by using data from long-screen boreholes. Britt (2005) used a sand tank borehole model to show that a long-screen monitoring borehole can create an artifact even when there is no vertical flow. In-well mixing occurs spontaneously and masks contaminant stratification in the aquifer. He also concluded that ground water stratification inside a borehole may not correspond to stratification at the same interval outside of the borehole.

All these works did not deal with the fresh water-salt water mixing zone monitored in observation boreholes in coastal aquifers where vertical gradients are significant.

Tidal Effects in Coastal Aquifers

The water table behaves as a traveling wave with periodicity similar to tide periodicity in response to tidal fluctuations (Nielsen 1990). As a tidal wave propagates inland through an aquifer, the damping effect progressively diminishes the amplitude of ground water head fluctuations (Carr and Van der Kamp 1969). The depth of the fresh water-salt water mixing zone is directly affected by the ground water head oscillations and it fluctuates (Strack 1976; Bear 1972; Wang and Tsay 2001). Underwood et al. (1992) showed that mixing of fresh water and salt water occurs primarily as a result of tidal fluctuations and depends to a lesser extent on dispersion processes. Tides influence the width of the fresh water-salt water mixing zone as well as the rate of ground water discharge (Robinson and Gallagher 1999; Uchiyama et al. 2000; Urish and McKenna 2004). Li et al. (1999) showed that tidal pumping and wave-induced circulation may constitute 96% of SGD. However, Michael et al. (2005) demonstrated that at their site tide-induced recirculation is not significant. However, Charette et al. (2005) and Robinson et al. (2007) illustrated that chemical flux to oceans is influenced by tide-induced recirculation. Cartwright et al. (2004) monitored temporal fluctuations in the fresh water-salt water mixing zone adjacent to the coastline. They used discrete pore water sampling spears and showed that fluctuations at their site were negligible in response to the tides. Kim et al. (2005) found that ground water quality is strongly connected to tides. The fresh water-salt water mixing zone fluctuates, and in high tides sea water might flow into pumping wells. Kim et al. (2006) measured ground water levels and the depth of the fresh water-salt water mixing zone at the coastal aquifer of Jeju Island, Korea. They showed that tidal effects on ground water levels reached up to 3 km inland from the coastline. Whereas Wang and Tsay (2001) demonstrated that the amplitude of the fresh water-salt water mixing zone fluctuations is similar to the amplitude of the water table fluctuations, Kim et al. (2006) measured the fresh water-salt water mixing zone fluctuation to be several meters in some places.

In the last two mentioned works (Kim et al. 2005, 2006), the monitoring wells were completely screened into the aquifers. As a result, bias observations caused by in-well flow might create these large mixing zone fluctuations.

Israel's Coastal Aquifer

Field work was conducted in Israel's coastal aquifer, along the Mediterranean coast, which is composed of interlayered sandstone, calcareous sandstone, siltstone, loam, and marine clays of Pleistocene age (Mualem and Bear 1974; Mercado 1980; Nativ and Weisbrod 1994). The coastal aquifer lies above an impermeable layer of shales called the Saqiye Group. The aquifer has a wedge-like shape, with a maximal thickness of 200 m beneath the coastline, and a minimal thickness of a few meters at the inland boundary. In several areas, as a result of overpumping during the past few decades, the fresh water–saline water interface has moved inland to a distance of more than 1 km (Bachmat and Chetboun 1974; Melloul and Gillad 1992). Hydraulic conductivity has been found by pumping tests (Mercado 2000), slug tests (Shalev and Hemo 2007), and numerical model calibration (Ben Shabat 1999).

The basic knowledge of the fresh water-salt water mixing zone is well supported by data from hundreds of long-screened boreholes (Hydrometric Department 1995; Vengosh et al. 1991; Yechieli et al. 1996) and from geophysical studies (TDEM, Goldman et al. 1991). Sorek et al. (2001) simulated sea water intrusion due to extensive pumping in the Gaza strip. Destouni and Prieto (2003) calculated SGD in the Nitzanim area although they were not able to verify their results with field measurements. Prieto and Destouni (2005) performed a two-dimensional simulation of tidal effects on the Israel coastal aquifer. However, because they did not have any data of the ground water fluctuations, saline/fresh water interface fluctuations, and SGD, they could not calibrate their results and their work remains theoretical. Moreover, two-dimensional simulations cannot truly represent ground water flow around wells and boreholes. When comparing field data to simulations, these issues become apparent because most of the data are collected from boreholes.

In this article, we aim to address the bias observation monitored in long-screen boreholes in the coastal aquifer of Israel.

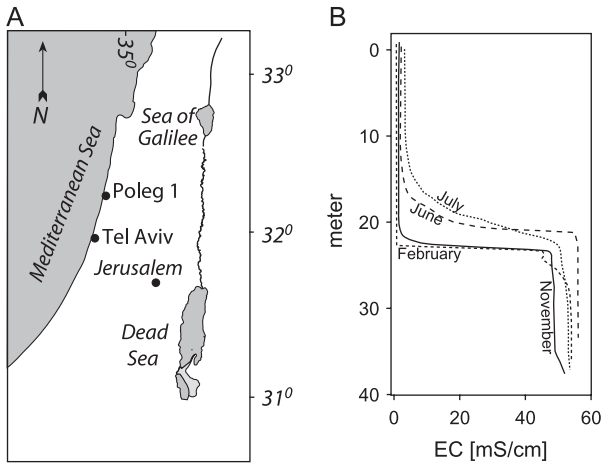

Figure 1. (A) Location of Poleg 1 borehole and (B) seasonal variations of the EC profiles.

Field Measurements

Water levels and EC profiles were measured at the Poleg 1 borehole, 20 km north of Tel-Aviv (Figure 1). This borehole is fully screened and is located 70 m from the shoreline. It is 47 m deep and the land elevation is 3.06 m above sea level. In this area, the aquifer is homogeneous and contains sandstone with only few thin layers of clay. These thin clay layers are considered to cause conductivity anisotropy of up to 1:30. As the EC of water is proportional to the solute concentration, the location of the mixing zone at this long-screen borehole is found by profiling the EC of the well (Lazar et al. 2003). A Hydrolab conductivity, temperature, and depth (CTD) diver was lowered into the borehole to generate a crude profile of the EC. At the first stage, the location of the mixing zone was determined, according to the sharp jump in conductivity. At the second stage, five CTD divers were placed at the transition zone with 1.75 m in-between the divers. Two additional divers were used to determine the hydraulic head in the borehole: one measuring pressure within the well and the other measuring barometric pressure outside the well (Lazar 2006).

Results of sea tide elevation, water table elevation, and EC at each of the five divers are shown in Figure 2. All have shown a clear fluctuation with periodicity corresponding to that of the sea tides. Using the EC data of the five divers, we calculated the depths of constant EC by linear interpolation (Figure 2). The data show that although sea level and ground water tidal amplitude are approximately 30 to 40 cm and 6 cm, respectively, the fresh water-salt water mixing zone amplitude is 1.5 m. These results contradict the theory according to which the fluctuations of both the water table and the mixing zone should be of the same magnitude (Wang and Tsay 2001). The measured high mixing zone fluctuations, which are probably a result of wellbore flow, are explained and modeled in the following sections.

Numerical Modeling and Discussion

The ground water tidal effects are modeled with FeFlow, a three-dimensional (3D) finite-element simulator (Diersch and Kolditz 2002) that solves the coupled variable density ground water flow and solute transport. Although the undisturbed ground water flow in a coastal aquifer can be simplified into a two-dimensional flow on a vertical cross section, the borehole introduces a radial flow with a component perpendicular to this cross section. Therefore, a 3D model is required for this problem. Flow boundary conditions are as follows: no flow on the west, bottom, north, and south plain boundaries; prescribed hydraulic head of 2.5 m above sea level on the east boundary; prescribed hydraulic head of the sea pressure on the sea floor; and free surface on the top land boundary. Salinity is prescribed on the sea floor (0.035 g/g) and on the right boundary (0 g/g). Therefore, the boundary condition head at the sea floor is

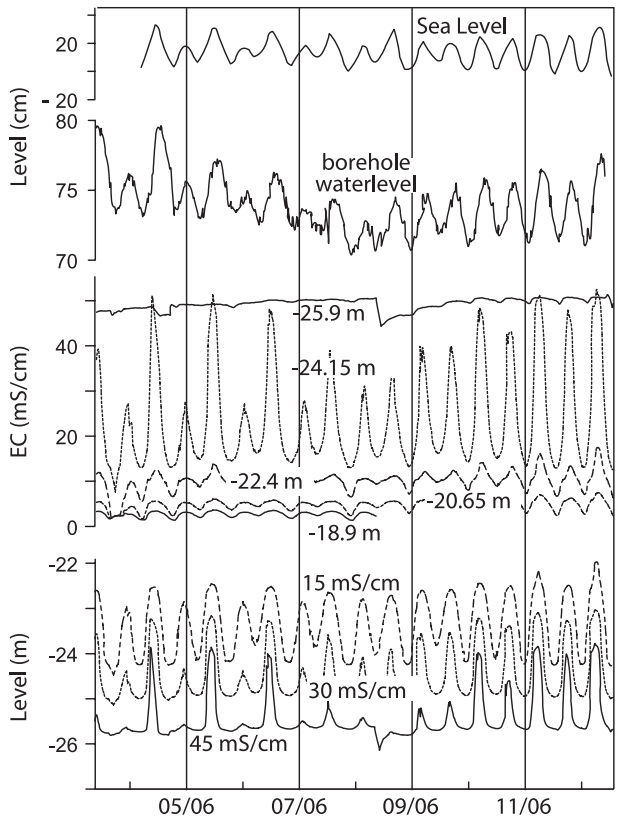

Figure 2. Top to bottom: sea level (data from Israel Limnological and Oceanographic Research), water level in the borehole, EC in five divers located in different depths in the borehole, and interpolated constant EC depths within the transition zone.

a function of the sea water depth times the water density. The borehole is simulated as a one-dimensional Hagen-Poiseuille flow line element (Diersch 2005) with a cross-sectional area of 0.1 m^2, effective hydraulic conductivity of 1 m/s, and longitudinal dispersivity coefficient of 0.1 m. Matrix hydraulic conductivity is 100 m/d, porosity is 0.2, specific storage is 10^{-4}/m, and longitudinal and transverse dispersivity coefficients are 10 and 1 m, respectively. The modeled grid was composed of 20 layers with 7451 elements per layer, totaling to 149,020 elements. For the transient simulations, the time steps were assigned to be 15 min.

Steady-State Simulation

The steady-state salinity distribution is shown in Figure 3. Fresh water flows from the right boundary and discharges at the sea floor. Sea water sinks down through the sea floor and discharges upward with the fresh water. Two cases are tested: (1) isotropic hydraulic conductivity and (2) vertical to horizontal hydraulic conductivities ratio of 1/30. Salinity distribution around the borehole is shown in Figure 4 for the anisotropic case. It is clearly shown that the borehole disturbs the natural flow and salinity distribution. Ground water flows up the borehole, transporting solutes as it ascends. Ground water with lower salinity enters the borehole at shallower depths and mixes with the ascending higher salinity ground water. The borehole affects only its immediate area (5 m) and no effects are noticeable at radial distances of more than 10 m from the borehole. A comparison between the isotropic and anisotropic cases is shown in Figure 5. Two main differences are demonstrated here. In the anisotropic case, the disturbance of the borehole is greater and fresh water discharges to the sea bottom further away from the shore.

In steady-state conditions, fresh water and salt water create a mixing zone and discharge together adjacent to the shoreline. In the anisotropic case, the vertical conductivity (3.3 m/d) is 30 times lower than the horizontal conductivity (100 m/d) reducing the upward discharge of the ground water. As the horizontal component of the ground water flow is higher than the vertical one, and all the ground water that flows horizontally is eventually discharged vertically, the mixing zone slope is smaller and the vertical flow is distributed over a larger area. As a result, the mixing zone is deeper and the SGD extends farther into the sea (Figure 5). Once the mixing zone is "punctured" by a borehole, ground water flows upward to the lower hydraulic head. The vertical hydraulic gradients are higher in the anisotropic case than in the isotropic case because the vertical hydraulic conductivity is lower. Therefore, the borehole interference is higher in the anisotropic case.

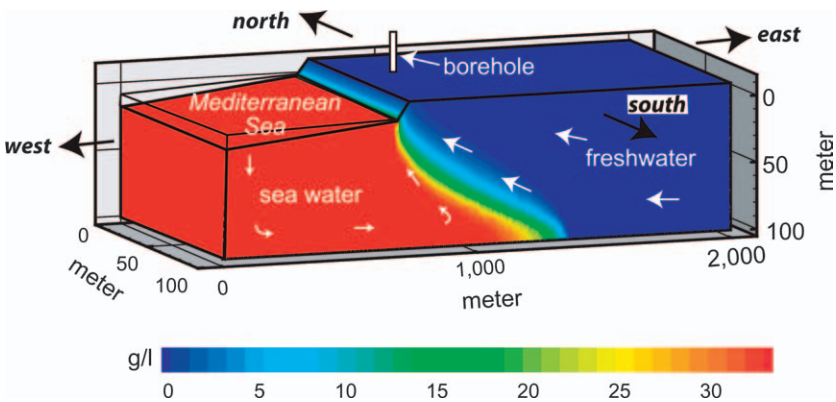

Figure 3. 3D simulation results of sea water intrusion showing classical salinity distribution at the fresh water-saline water mixing zone.

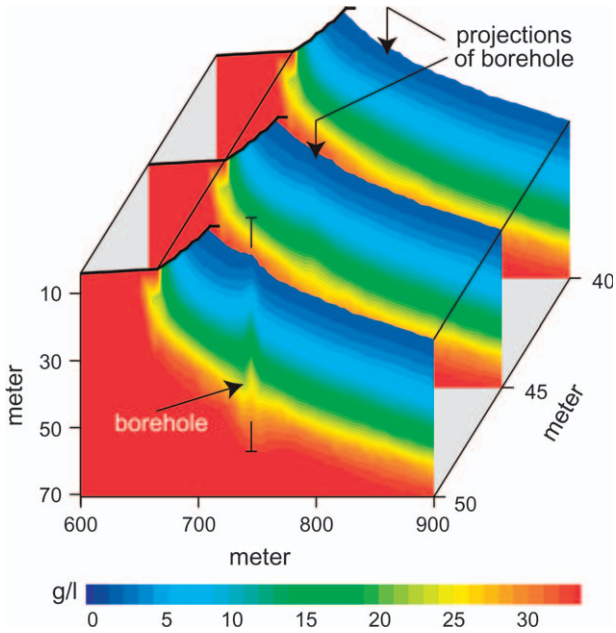

Figure 4. Simulation results showing salinity distribution around the borehole for the anisotropic case. The borehole affects the natural flow and elevates the fresh water-salt water mixing zone. Away from the borehole, the natural flow is undisturbed.

The effective hydraulic conductivity of the borehole assuming Hagen-Poiseuille flow is $r^2\rho g/8\mu$, where r is the borehole radius, ρ ground water density, g acceleration due to gravity, and μ ground water viscosity. Substituting the borehole values into these equations gives an effective conductivity of 781 m/s. As, expected, a greater effective conductivity causes a greater wellbore flow. However, this high value caused some numerical instability in our simulation. We, therefore, examined also the situation when using lower values by 1 to 2 orders of magnitude. Sensitivity analysis shows that the difference between using a value of 781 m/s and a value of 1 m/s is not significant. In both cases, the wellbore effect is very large. Therefore, we used the more numerically stable value of 1 m/s in our simulations.

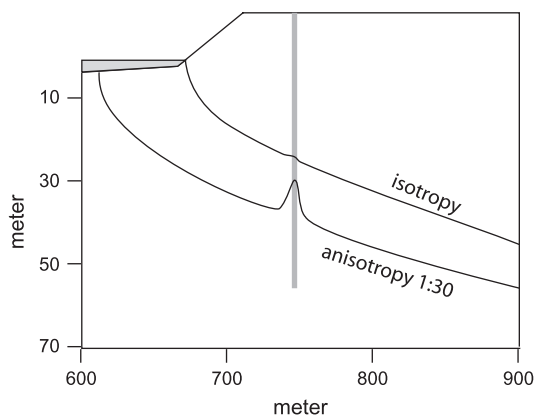

Figure 5. A comparison between the locations of the 50% sea water isopleth of the isotropic and anisotropic cases in steady-state conditions.

Tidal Effects

In the following simulations, the sea level is continuously changed in a sinusoidal manner with amplitude of 40 cm. Water table and 50% sea water isopleths fluctuations in the borehole for both cases are shown in Figure 6. The amplitudes of both are higher in the case of isotropic hydraulic conductivity. The simulated mixing zone fluctuations of 140 cm for isotropic conditions produce a better fit to the field observations than the 60 cm of the anisotropic simulations.

The hydraulic head behaves as a traveling wave in response to tidal fluctuations. As a result, ground water flow field changes, and the fresh water-salt water mixing zone also fluctuates. Once the traveling wave reaches the borehole and changes the hydraulic head, the mixing zone responds almost instantaneously because of the high hydraulic conductivity of the borehole.

The amplitude of the traveling head wave depends on the hydraulic conductivity. The lower the conductivity is, the higher the damping effect that diminishes the amplitude of ground water head. The wave propagates in all directions. In the anisotropic case, since the vertical hydraulic conductivity is smaller than the horizontal conductivity, the effective conductivity is smaller in any diagonal direction. Therefore, the overall effective hydraulic conductivity in the isotropic case is greater than the conductivity in the anisotropic case, resulting in smaller damping and higher amplitude in the isotropic case.

Figure 7 shows that all these high fluctuations of the mixing zone occur only within the borehole and its immediate vicinity (less than 10 m), while beyond that the changes are only few centimeters. The existence of the borehole affects only the mixing zone fluctuations and

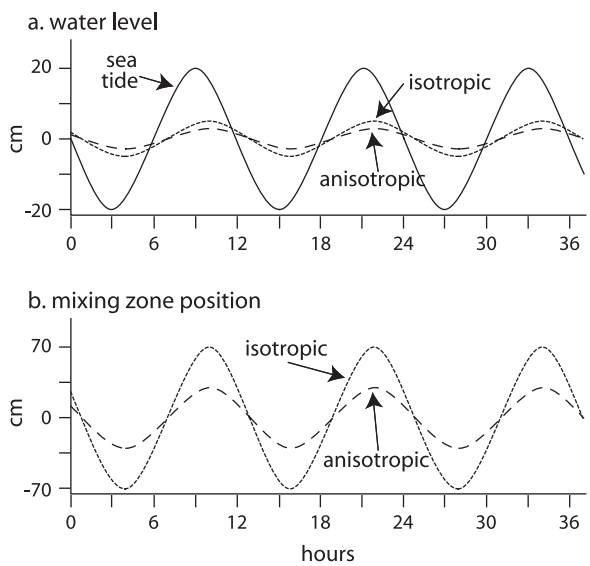

Figure 6. Simulation results showing the boundary condition sea tide, resulting water table in the borehole for both isotropic and anisotropic cases (top), and resulting 50% sea water isopleth for both isotropic and anisotropic cases in the borehole. The 50% sea water isopleth amplitudes are significantly higher than the water table amplitudes. Datum levels are the mean values of each.

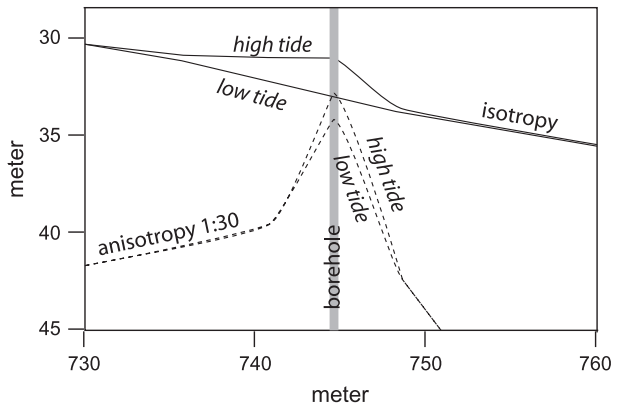

Figure 7. A comparison between the locations of the 50% sea water isopleths of the isotropic case and the anisotropic case with high and low sea tides.

not the water table fluctuations. When there is no borehole, the magnitude of the mixing zone fluctuations is only few centimeters. As mentioned in the previous section, the oscillating hydraulic head changes the ground water flow pattern and the fresh water–salt water mixing zone location. In the borehole, since the hydraulic conductivity of the borehole is high, any change of the hydraulic head will significantly change the ambient flow. Outside of the borehole, where hydraulic conductivity is much lower, so are the ground water velocities. Since the fresh water-salt water mixing zone is affected by ground water velocity, its response to tides is larger in the borehole where velocity changes are higher than outside of the borehole where velocity changes are low. The fluctuations of the 50% sea water isopleths are larger for the isotropic case than the anisotropic case because the upward background steady-state flow through the borehole is higher for the anisotropic case (larger vertical hydraulic gradient). Having the same magnitude of flow fluctuation on a different background flow will be more significant when the background flow is small.

Figure 8 shows equivalent fresh water hydraulic head, salinity, and ground water velocity on the borehole plane perpendicular to the coast line. The velocity scales are different in the borehole and outside the borehole. These results are also shown in the animation provided in the attached Supporting Information with a better time resolution. Although the amplitude of the fresh water hydraulic head fluctuation is only 20 cm, ground water velocity changes significantly. The fresh water-salt water mixing zone fluctuates for similar amplitude and it is not noticed in this scale. At the lower part of the cross section that contains the salt water, the flow changes its direction by 180° during a cycle. The downward flow component created during low tides (Figure 8B) is reversed during high tides (Figure 8D). Each of these flow patterns lasts for no more than 6 h before it returns to the previous pattern. As a result, water flow within the borehole is upward during a high sea level and downward during a low sea level. Because flow velocity in the borehole is more than 3 orders of magnitude higher than the flow outside the borehole, the effect of the

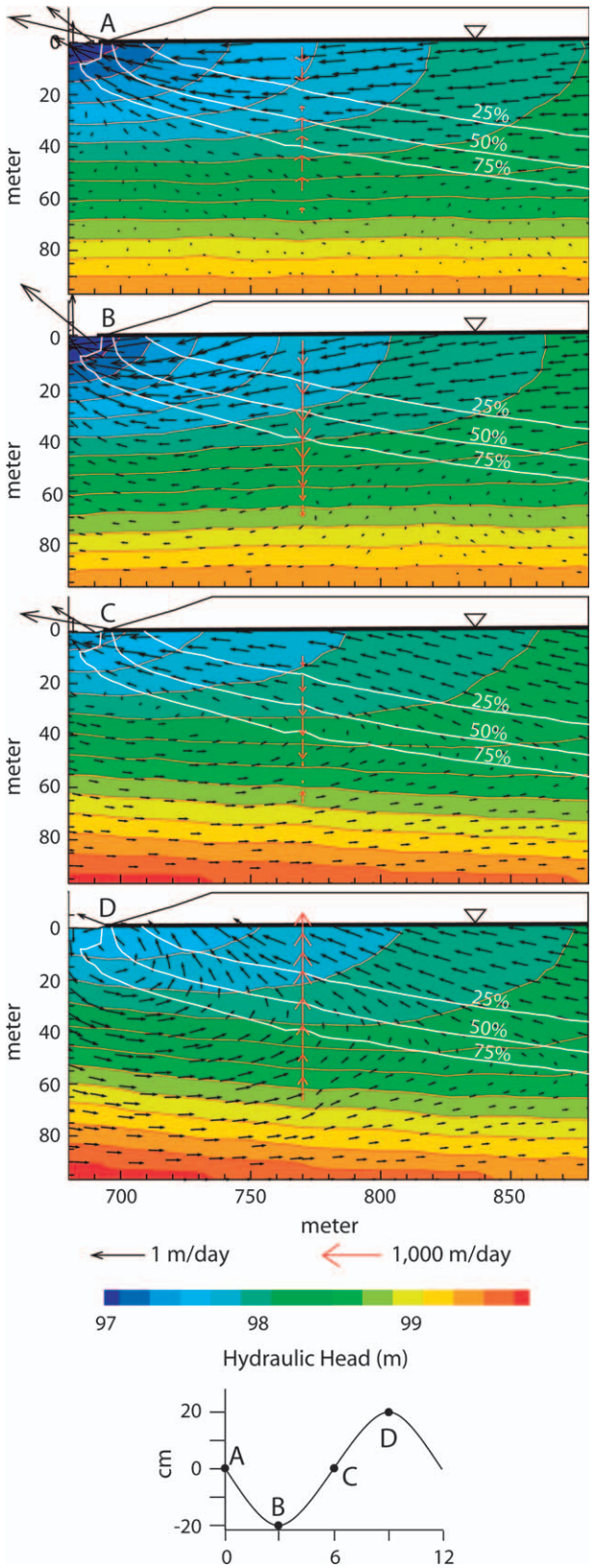

Figure 8. Simulation results of the effects of a 12-h sea tide cycle on ground water in an isotropic aquifer. Equivalent fresh water hydraulic head is colored and ground water salinity isopleths are marked by white lines. Note that the scale of the velocity vector within the borehole is 1000 times larger than the velocity vector outside the borehole.

flow on the fresh water-salt water mixing zone is higher within the borehole itself. Because ground water is eventually discharging to the coast, the average flow within the borehole is also upward as in the steady-state conditions (Figure 5). The fluctuations of the isopleths within the borehole created by tides are about the steady-state conditions (Figure 7). While water is flowing through the screened borehole, its salinity is dispersed with ground water around the borehole, dampening the salinity signal. As a result, even when the flow within the borehole is downward, the isopleths still have a local maximum at the borehole.

Conclusions

Although the fresh water-sea water mixing zone has been studied and modeled by numerous researchers, we add herein a new piece of information, which is highlighted by Figure 8 and by the attached animation (an electronic Supporting Information for the article). With this modeling, we are able to accurately describe the biased monitoring of a fully screened observation well, in which the fluctuation magnitude of the mixing zone is an order of magnitude larger than that in the porous media.

Field measurements and numerical modeling show that observations monitored in long-screen boreholes do not accurately represent natural phenomena. The approximately 500 monitoring boreholes in the coastal aquifer of Israel do not accurately monitor the actual fresh water–salt water mixing zone. Boreholes may act as a short circuit along a vertical gradient, connecting between the higher and lower hydraulic head zones. As a result, flow in the well is often large enough to compromise the integrity of water samples. This is shown to occur in coastal aquifers both in steady-state and transient (tide) conditions. The main parameters that affect the magnitude of this biased observation are the anisotropy of the hydraulic conductivity and the difference between the aquifer and borehole hydraulic parameters (borehole hydraulic conductivity depends on its diameter).

In steady-state conditions, the borehole interference is higher for the anisotropic case because the vertical hydraulic gradients are higher in the anisotropic case than in the isotropic case. When tides are introduced, the amplitude of the mixing zone fluctuation is higher for the isotropic case because the overall effective hydraulic conductivity in the isotropic case is greater than the conductivity in the anisotropic case. The high amplitude of the fresh water-salt water mixing zone occurs only in the borehole. In the aquifer, the fresh water-salt water mixing zone fluctuations are dampened, and tens of meters inland from the shoreline, the fluctuations are on the order of few centimeters.

Acknowledgments

This study was financed by the Israeli Water Commission. We thank Dov Rosen from the Israel Oceanography and Limnological Research for supplying the data of sea level fluctuations. We thank the five reviewers, Dr. Pierre Lacombe, Dr. Kue-Young Kim, and Dr. Juliette Woods, as well as the two additional anonymous reviewers, for thorough evaluations of the manuscript.

Supporting Information

Additional Supporting Information may be found in the online version of this article:

Animation S1. An animation of simulation results on the effects of a 12-h sea tide cycle on ground water in an isotropic aquifer. Fresh water hydraulic head is colored and ground water salinity isopleths are marked by white lines. The scale of the velocity within the borehole is 1000 times larger than the velocity outside the borehole.

Please note: Wiley-Blackwell are not responsible for the content or functionality of any supporting materials supplied by the authors. Any queries (other than missing material) should be directed to the corresponding author for the article.

References

Bachmat, Y., and G. Chetboun. 1974. Sea water encroachment in the Coastal Plain of Israel during the period 1958-1971. Hydrological Service Report 74/2. Jerusalem, Israel: Water Commission.

Bear, J. 1972. *Dynamics of Fluids in Porous Media*. New York: American Elsevier.

Ben Shabat, J. 1999. EWRE, two dimensional simulation of the coastal aquifer; part 1 (in Hebrew). Haifa, Israel: EWRE.

Britt, S.L. 2005. Testing the in-well horizontal laminar flow assumption with a sand-tank well model. *Ground Water Monitoring Remediation* 25, no. 3: 73–81.

Carr, P.A., and G.S. Van der Kamp. 1969. Determining aquifer characteristics by the tidal method. *Water Resources Research* 5, no. 5: 1023–1031.

Cartwright, N., L. Li., and P. Nielsen. 2004. Response of the salt-freshwater interface in a coastal aquifer to a wave-induced groundwater pulse: Field observations and modeling. *Advances in Water Resources* 27: 297–303.

Charette, M.A., E.R. Sholkovitz, and C.M. Hansel. 2005. Trace element cycling in a subterranean estuary: Part 1. Geochemistry of permeable sediments. *Geochimica et Cosmochimica Acta* 69: 2095–2109.

Church, P.E., and G.E. Granato. 1996. Bias in ground-water data caused by well-bore flow in long-screen wells. *Ground Water* 34, no. 2: 262–273.

Diersch, H.-J.G. 2005. *FeFlow—Finite Element Subsurface Flow and Transport Simulation System*. Reference manual. Berlin, Germany: WASY GmbH.

Destouni, G., and C. Prieto. 2003. On the possibility for generic modeling of submarine groundwater discharge. *Biogeochemistry* 66: 171–186.

Diersch, H.-J.G., and O. Kolditz. 2002. Variable-density flow and transport in porous media: Approaches and challenges. *Advances in Water Resources* 25: 899–944.

Elci, A., P.F. Gregory, and F.J. Molz. 2003. Detrimental effects of natural head gradients on chemical and water level measurements in observation wells: Identification and control. *Journal of Hydrology* 281: 70–81.

Elci, A., F.J. Molz, and W.R. Waldrop. 2001. Implications of observed and simulated ambient flow in monitoring wells. *Ground Water* 39, no. 6: 853–862.

Giddings, T. 1987. What is an adequate screen length for monitoring wells? Option 1. *Ground Water Monitoring Review* 7, no. 2: 96–97.

Goldman, M., D. Gilad, A. Ronen, and A. Melloul. 1991. Mapping of seawater intrusion into the coastal aquifer of Israel by the time domain electromagnetic method. *Geoeploration* 28: 153–174.

Hutchins, S.R., and S.D. Acree. 2000. Ground water sampling bias observed in shallow, conventional wells. *Ground Water Monitoring Remediation* 20, no. 1: 86–93.

Hydrometric Department. 1995. Development, exploitation and groundwater resources in Israel till autumn 1995 (in Hebrew). Jerusalem, Israel: Hydrometric Department.

Kim, J.H., J. Lee, T.J. Cheong, R.H. Kim, D.C. Koh, J.S. Ryu, and H.W. Chang. 2005. Use of time series analysis for the identification of tidal effect on groundwater in the coastal area of Kimje, Korea. *Journal of Hydrology* 300: 188–198.

Kim, K.Y., H. Seong, T. Kim, K.H. Park, N.C. Woo, Y.S. Park, G.W. Koh, and W.B. Park. 2006. Tidal effects on variations of fresh-saltwater interface and groundwater flow in a multilayered coastal aquifer on a volcanic island (Jeju Island, Korea). *Journal of Hydrology* 330: 525–542.

Konikow, L.F., and G.Z. Hornberger. 2006. Modeling effects of multimode wells on solute transport. *Ground Water* 44, no. 5: 648–660.

Lacombe, S., E.A. Sudicky, S.K. Frape, and A.J.A. Unger. 1995. Influence of leaky boreholes on cross-formational groundwater flow and contaminant transport. *Water Resources Research* 31, no. 8: 1871–1882.

Lazar, A. 2006. Tidal and seasonal variations of the fresh-saline water interface and water level in the coastal aquifer of Israel. Geological Survey of Israel Report GSI/04/2006. Jerusalem, Israel: Geological Survey of Israel.

Lazar, A., H. Gvirtzman, and Y. Yechieli. 2003. Tidal effects on fresh-saline interface fluctuations in coastal aquifers. Conference on Saltwater Intrusion and Coastal Aquifers: Monitoring, Modeling and Management, México.

Li, L., D.A. Barry, F. Stagnitti, and J.-Y. Parlangeand. 1999. Submarine groundwater discharge and associated chemical input to a coastal sea. *Water Resources Research* 35: 3253–3260.

Melloul, A., and D. Gillad. 1992. Importance of the seawater interface monitoring network for the coastal aquifer. Hydrological Service Report Hydro/1992/4. Jerusalem, Israel: Hydrological Service.

Mercado, A. 2000. Hydrological assessment of the alternative of sea water supply to desalination plants through wells in the southern coastal plain; progress report number 2 (in Hebrew).

Mercado, A. 1980. The coastal aquifer of Israel, some quality aspects of groundwater management. In *Water Quality Management under Conditions of Scarcity*, ed. H.I. Shuval, 93–146. New York: Academic Press.

Michael, H.A., A.E. Mulligan, and C.F. Harvey. 2005. Seasonal oscillations in water exchange between aquifers and the coastal ocean. *Nature* 436: 1145–1148.

Mualem, Y., and J. Bear. 1974. The shape of the interface in steady flow in a stratified aquifer. *Water Resources Research* 10: 1207–1215.

Nativ, R., and N. Weisbrod, 1994. Hydraulic connections among sub-aquifers of the Coastal Plain Aquifer, Israel. *Ground Water* 32, no. 6: 997–1007.

Nielsen, P. 1990. Tidal dynamics at water table in beaches. *Water Resources Research* 26: 2127–2134.

Prieto, C., and G. Destouni. 2005. Quantifying hydrological and tidal influences on groundwater discharges into coastal waters. *Water Resources Research* 41, W12427.

Reilly, T.E., O.L. Franke, and G.D. Bennett. 1989. Bias in groundwater samples caused by wellbore flow. *Journal of Hydraulic Engineering* 115, no. 2: 270–276.

Robbins, G.A. 1989. Influence of using purged and partially penetrating monitoring wells on contaminant detection, mapping, and modeling. *Ground Water* 27: 155–162.

Robinson, C., L. Li, and D.A. Barry. 2007. Effect of tidal forcing on a subterranean estuary. *Advances in Water Resources* 30: 851–865.

Robinson, M.A., and D.L. Gallagher. 1999. A model of ground water discharge from an unconfined coastal aquifer. *Ground Water* 37, no. 1: 80–87.

Shalev, E., and Hemo, H. 2007. Slug tests performed at the Coastal Plain Aquifer. Geological Survey of Israel Report, GSI/10/2007 (in Hebrew).

Shosky, D.J. Jr. 1987. What is an adequate screen length for monitoring wells? Option 2. *Ground Water Monitoring Review* 7, no. 2: 98–103.

Sorek S., V.S. Borisov, and A. Yakirevich. 2001. A two-dimensional areal model for density dependent flow regime. *Transport in Porous Media* 43, no. 1: 87–105.

Strack, O.D.L. 1976. A single-potential solution for regional interface problems in coastal aquifers. *Water Resources Research* 12, no. 6: 1165–1174.

Sukop, M.C. 2000. Estimation of vertical concentration profiles from existing wells. *Ground Water* 38, no. 6: 836–841.

Uchiyama, Y., K. Nadaoka, P. Rölke, K. Adachi, and H. Yagi. 2000. Submarine groundwater discharge into the sea and associated nutrient transport in a sandy beach. *Water Resources Research* 36, no. 6: 1467–1480.

Underwood, M.R., F.L. Peterson, and C.I. Voss. 1992. Groundwater lens dynamics of atoll islands. *Water Resources Research* 28, no. 11: 2889–2902.

Urish, D.W., and T.E. McKenna. 2004. Tidal effects on ground water discharge through a sandy marine beach. *Ground Water* 42, no. 7: 971–982.

Vengosh, A., A. Starinsky, A. Melloul, M. Fink, and S. Erlich. 1991. Salinization of the coastal aquifer water by Cachloride solutions at the interface zone, along the Coastal Plain of Israel. Hydrological Service Report Hydro/20/1991 (in Hebrew). Jerusalem, Israel: Hydrological Service.

Wang, J., and T.K. Tsay. 2001. Tidal effects on groundwater motions. *Transport in Porous Media* 43: 159–178.

Yechieli, Y., D. Ronen, and A. Vengosh. 1996. Preliminary 14C study of groundwater at the fresh-saline water interface of the Mediterranean coastal plain aquifer in Israel. In *Proceedings of the 14th Salt Water Intrusion Meeting*, 84–90. Malmo, Sweden.